Available online at www.sciencedirect.com
SCIENCE DIRECT®
International Journal of Plasticity 22 (2006) 1171–1194
INTERNATIONAL JOURNAL OF Plasticity
www.elsevier.com/locate/ijplas

Orthotropic yield criterion for hexagonal closed packed metals

Oana Cazacu [a,*], Brian Plunkett [a], Frédéric Barlat [b]

[a] *Department of Mechanical and Aerospace Engineering, University of Florida's Graduate Engineering and Research Center, Shalimar, FL 32579-1163, USA*
[b] *Materials Science Division, Alcoa Inc., Alcoa Technical Center, 100 Technical Drive, Alcoa Center, PA 15069-0001, USA*

Received 2 April 2005
Available online 11 October 2005

Abstract

In this paper, a macroscopic orthotropic yield criterion, which can describe both the anisotropy of a material and the yielding asymmetry between tension and compression, is introduced. The yield function is expressed in terms of the principal values of the stress deviator, ensuring insensitivity to the hydrostatic pressure. Application of the proposed criterion to magnesium and titanium alloy sheets shows that this model can capture very well the complex behavior of these materials.

Keywords: Plastic anisotropy; Twinning; Tension–compression asymmetry; Hexagonal closed packed metals

1. Introduction

Hexagonal closed packed (hcp) metals and alloys are important to nearly every modern industry, ranging from biomedical applications, such as Ti implants and NiTi superelastic catheter guides; to new Sn-based lead-free solders under explora-

* Corresponding author. Tel.: +1 850 833 9350; fax: +1 850 833 9366.
E-mail address: cazacu@gerc.eng.ufl.edu (O. Cazacu).

0749-6419/$ - see front matter
doi:10.1016/j.ijplas.2005.06.001

tion by the microelectronics industry; to Ti (or TiAl) alloy jet engine compressor components. These advanced materials have excellent properties for their target applications (e.g., Ti implants exhibit biocompatibility, light weight, high strength, and low stiffness); however, their use is still limited because of problems associated with poor formability and consequently high manufacturing costs (see for example, Avedesian and Baker, 1999; Takuda et al., 1999). Traditional explanations of these phenomena relate to the fact that most cold-rolled hcp alloy sheets have basal or nearly basal textures, i.e., the ***c***-axis is aligned normal to the plane of the sheet. A degree of spread from this ideal texture by up to $\pm 20°$ about the transverse direction is observed for magnesium while for alpha titanium and zirconium alloys the spread is up to 40° (see Hosford, 1966). Depending on the c/a ratio, either prism slip or basal slip along the closed-packed basal directions $\langle a\rangle$ generally dominates the plastic response. Slip on pyramidal planes along the a-directions is significantly harder, and even more difficult on the pyramidal planes along the $\langle c+a\rangle$ directions. However, basal slip does not produce any elongation or shortening parallel to the ***c***-axis. Thus, only twinning or pyramidal slip can accommodate inelastic shape changes in the c-direction. For most hcp metals, the most easily activated twinning mode is the tensile twin $\{1\,0\,1\,2\}\langle 1\,0\,\bar{1}\,1\rangle$, which is not activated by tension in the plane of the sheet. Because of the directionality of twinning, at low strain levels a very pronounced strength differential (SD) effect is observed: the compressive strengths are much lower than the tensile strengths (Hosford, 1993; Tomé et al., 2001; etc.). At high strain levels, when twinning has practically ceased, this asymmetry is markedly diminished. Since the pyramidal slip and compression twinning are much harder than the primary deformation modes of basal slip and tension twinning, most hcp sheets display a strong resistance to thinning. For example, for textured magnesium sheets values of 2–4.5 of the ratio r of the width strain-to-thickness strain are commonly observed (Agnew and Duygulu, 2005; Kaiser et al., 2003) while for titanium values as high as 9 have been reported (see Hosford, 1993).

A general framework for description of yielding anisotropy and its evolution with accumulated deformation is offered by polycrystal viscoplasticity. Direct polycrystal viscoplasticity implementation in which a representation of the texture is embedded within every finite element and the stress and stiffness needed are computed using the equations for the single crystal response and the associated interaction law (linking hypothesis) has the advantage that it follows the evolution of anisotropy due to texture changes. However, the correct modeling of the strong asymmetry between tension and compression due to deformation twinning remains a challenge. As discussed by Van-Houtte (1978) and Tomé et al. (1991), a major obstacle in extending the crystal plasticity framework to include deformation twinning is the difficulty in handling the large number of orientations created by twinned regions. Although progress has been made and models that track the evolution of the twinned regions in the grain and account for predominant twin reorientation (e.g., Tomé and Lebensohn, 2004) or intergranular mechanisms (e.g., Staroselsky and Anand, 2003) have been proposed, the use of such models is still limited because the calculations are computationally very intensive even for problems that do not require a fine spatial resolution. Phenomenological descriptions of plastic anisotropy are convenient and timeefficient for sheet forming process simulations. However, in contrast to the recent progress in the formulation, numerical implementation, and validation of macroscopic plasticity models for materials with cubic structure (e.g., Barlat et al., 2003, 2004, 2005; Cazacu and Barlat, 2003; Bron and Besson, 2004, etc.), modeling of hcp materials is less developed. Due to the lack of adequate macroscopic criteria for hcp materials, hcp sheet forming FEM simulations are still performed using classic anisotropic formulations for cubic metals such as Hill (1948) (see for example, Takuda et al., 1999; Kuwabara et al., 2001). There is a clear need to develop physically based macroscopic level anisotropic formulations that could describe *both the anisotropy and asymmetry in yielding (tension vs. compression) of hcp metals* and that can be easily implemented in FE element codes and thus applicable routinely to the simulation of sheet forming processes.

To account for initial plastic anisotropy or to describe an average material response over a certain deformation range, rigorous methods have been proposed in the literature (e.g., the linear transformation approach proposed by Barlat et al. (1991) and Karafillis and Boyce (1993); the generalized invariants approach proposed by Cazacu and Barlat (2001, 2003)). The major difficulty encountered in formulating analytic expressions for the yield functions of hcp metals is related to the description of the SD effect (tension vs. compression asymmetry).

The purpose of this paper is to propose a general, physically based and numerically robust macroscopic formulation that describes with accuracy *both the asymmetry and anisotropy in yielding exhibited by hcp materials*. The approach that will be adopted is: (1) to develop macroscopic isotropic yield function that could describe in a realistic manner non-symmetrical yielding effects (tension vs. compression) based on single and polycrystalline viscoplasticity; (2) to extend the isotropic formulation such as to account for orthotropy. The validity of the proposed model is demonstrated through comparison between calculated and experimental yield loci for sheets of textured polycrystalline binary Mg–Th and Mg–Li alloys (data after Kelley and Hosford, 1968) and α Titanium (data after Lee and Backofen, 1966).

2. Proposed isotropic yield criterion for description of asymmetric yielding

If a material only deforms by a reversible shear mechanism such as slip, yielding depends only on the magnitude of the resolved shear stress. Thus, the yield locus in the deviatoric π plane (plane which passes through the origin and is perpendicular to the hydrostatic axis) must have sixfold symmetry. The shape of the yield surface of such an isotropic material is dictated by the requirements of: (a) pressure-independence; (b) invariance with respect to any transformation belonging to the orthogonal group; (c) equal yield stresses in tension and compression. The size of the yield locus is determined quite effectively by observing when yielding occurs in a few tests, such as a tension test or a pure shear test. Yielding of such materials is thus represented by an even function of the principal values of the stress deviator, $\boldsymbol{S}$.

Twinning and martensitic shear are directional deformation mechanisms, and if they occur, yielding will depend on the sign of the stress (Hosford, 1993). Early simulations results by Chin et al. (1969), who analyzed deformation by mixed slip and twining in fcc crystals, predicted a yield stress in uniaxial tension 25% lower than that in uniaxial compression. Hosford and Allen (1973) extended the calculations to other types of loading. Based on the simulation results they concluded that yield loci with a strong asymmetry between tension and compression should be expected in any isotropic pressure insensitive material that deforms by twinning or directional slip. Based on the shape of the yield locus obtained through polycrystalline simulations by Hosford and Allen (1973), Cazacu and Barlat (2004) proposed an isotropic yield criterion of the form

$$f \equiv (J_2)^{\frac{3}{2}} - cJ_3 = \tau_Y^3, \tag{1}$$

where $J_2 = \mathrm{tr}\boldsymbol{S}^2/2$ and $J_3 = \mathrm{tr}\boldsymbol{S}^3/3$ are the second and third invariants of the stress deviator $\boldsymbol{S}$, respectively (tr denotes the trace operator), i.e., $\mathrm{tr}(\boldsymbol{A}) = \sum_{k=1}^{3} A_{kk}$; τ_Y is the yield stress in pure shear and c is a material constant expressible solely in terms of σ_T and σ_C the uniaxial yield stresses in tension and compression

$$c = \frac{3\sqrt{3}(\sigma_\mathrm{T}^3 - \sigma_\mathrm{C}^3)}{2(\sigma_\mathrm{T}^3 + \sigma_\mathrm{C}^3)}. \tag{2}$$

Note that for equal yield stresses in tension and compression $c = 0$, hence the proposed criterion reduces to the von Mises yield criterion. For the yield function (1) to be convex, the constant c is limited to a given numerical range: $c \in [-3\sqrt{3}/2, 3\sqrt{3}/4]$.

For plane stress conditions, the yield locus is given by

$$\left[\frac{1}{3}(\sigma_1^2 - \sigma_1\sigma_2 + \sigma_2^2)\right]^{3/2} - \frac{c}{27}\left[2\sigma_1^3 + 2\sigma_2^3 - 3(\sigma_1 + \sigma_2)\sigma_1\sigma_2\right] = \tau_Y^3, \tag{3}$$

where σ_1 and σ_2 denote the principal stresses. For any $c \neq 0$, the yield function is homogeneous of degree 3 in stresses and Eq. (3) represents a "triangle" with rounded corners. As an example, in Fig. 1 are shown the plane stress yield loci (3) corresponding to $\sigma_\mathrm{T}/\sigma_\mathrm{C} = 2/3$, 1 (von Mises), and 3/2, respectively.

In this paper, we introduce a new isotropic yield criterion of the form

$$(|S_1| - kS_1)^a + (|S_2| - kS_2)^a + (|S_3| - kS_3)^a = F, \tag{4}$$

where S_i, $i = 1,\ldots,3$ are the principal values of the stress deviator. At difference with the yield criterion (3), the proposed yield function (4) is a homogeneous function of degree a in stresses. The exponent a is considered to be a positive integer. Also, in (4) k is a material constant, while F gives the size of the yield locus and may be considered either constant (rigid plastic response) or function of the accumulated plastic strain (isotropic hardening). The physical significance of the material parameter k may be revealed from uniaxial tests. Indeed, according to the proposed criterion (4), the ratio of tensile to compressive uniaxial yield stress is given by

$$\frac{\sigma_\mathrm{T}}{\sigma_\mathrm{C}} = \left\{\frac{\left(\frac{2}{3}\cdot(1+k)\right)^a + 2\cdot\left(\frac{1}{3}\cdot(1-k)\right)^a}{\left(\frac{2}{3}\cdot(1-k)\right)^a + 2\cdot\left(\frac{1}{3}\cdot(1+k)\right)^a}\right\}^{\frac{1}{a}} \tag{5a}$$

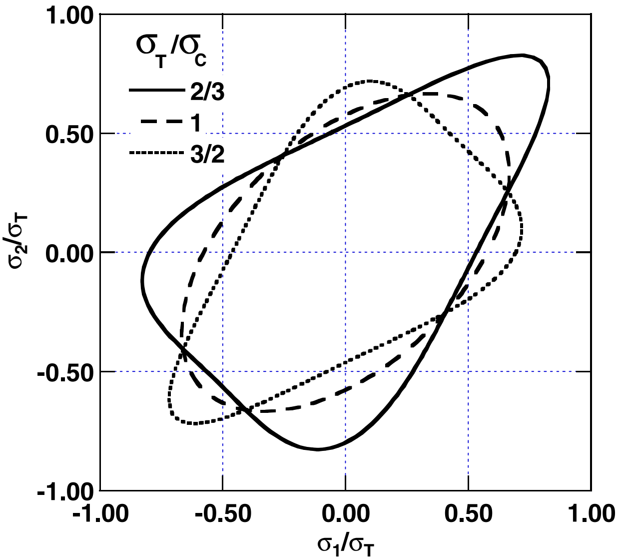

Fig. 1. Plane-stress yield loci according to Cazacu and Barlat (2004) criterion for different values of the ratio $\frac{\sigma_T}{\sigma_C}$ between the yield stress in tension and compression, in comparison with the Von Mises yield locus (σ_1 and σ_2 are the principal values of the Cauchy stress).

or

$$k = \frac{1 - h\left(\frac{\sigma_T}{\sigma_C}\right)}{1 + h\left(\frac{\sigma_T}{\sigma_C}\right)} \tag{5b}$$

with

$$h\left(\frac{\sigma_T}{\sigma_C}\right) = \left[\frac{2^a - 2\left(\frac{\sigma_T}{\sigma_C}\right)^a}{\left(2\frac{\sigma_T}{\sigma_C}\right)^a - 2}\right]^{\frac{1}{a}}. \tag{5c}$$

Hence, for a fixed, the parameter k is expressible solely in terms of the ratio $\frac{\sigma_T}{\sigma_C}$ (see (5b) and (5c)). Note that for any value of $a \geqslant 1$,a integer if $k = 0$, there is no difference between the response in tension and compression. In particular, for $k = 0$ and $a = 2$, the proposed criterion reduces to the von Mises yield criterion. From (5b) follows that for a given exponent "a", for the parameter k to be real,

$$2^{\frac{1-a}{a}} \leqslant \frac{\sigma_T}{\sigma_C} \leqslant 2^{\frac{a-1}{a}}. \tag{6}$$

Specifically:

- for $2^{\frac{1-a}{a}} \leqslant \frac{\sigma_T}{\sigma_C} \leqslant 1 \Rightarrow -1 \leqslant k \leqslant 0$,
- for $1 \leqslant \frac{\sigma_T}{\sigma_C} \leqslant 2^{\frac{a-1}{a}} \Rightarrow 0 \leqslant k \leqslant 1$.

As an example, in Fig. 2 are shown the representation of the plane stress yield loci (4) corresponding to $a = 2$ (fixed) and $\sigma_T/\sigma_C = \sqrt{2}$, 1.26, 1.13 and 1 (von Mises), respectively (i.e., corresponding to $k = 1$; 0.4; 0.2; 0, respectively). Note that the higher the ratio between the yield stress in tension and compression, the greater is the departure from the von Mises ellipse; for the highest admissible value for k, the yield function (4) represents a triangle with rounded corners.

Furthermore, since $h(\frac{1}{x}) = \frac{1}{h(x)}$, it follows that $k(\frac{\sigma_T}{\sigma_C}) = -k(\frac{\sigma_C}{\sigma_T})$ (see Eqs. (5)). To illustrate this property of the proposed yield function, in Fig. 3 are represented the plane stress yield loci (4) corresponding to $\sigma_T/\sigma_C = 1.13$ ($k = 0.2$) and $\sigma_T/\sigma_C = 1/1.13$ ($k = -0.2$). It is clearly seen that a change in the sign of k results in a mirror image of the yield surface. The variation of $\frac{\sigma_T}{\sigma_C}$ with k is illustrated in Fig. 4 for different values of the exponent a. If $k = 1$ then $\frac{\sigma_T}{\sigma_C} = 2^{\frac{a-1}{a}}$ so for $a = 1$: $\sigma_T = \sigma_C$, while for $a \to \infty$, $\frac{\sigma_T}{\sigma_C} \to 2$: if $k = -1$: $\frac{\sigma_T}{\sigma_C} = 2^{\frac{1-a}{a}}$, so for $a = 1$ there is no difference between tension and compression, while if $a \to \infty$, then $\frac{\sigma_T}{\sigma_C} \to \frac{1}{2}$. For any integer $a \geqslant 1$ and for $-1 \leqslant k \leqslant 1$, the yield function (4) is convex (for the proof, see Appendix A).

For combined tension and torsion conditions where the uniaxial tensile stress is set equal to σ, the shear stress is set equal to τ, and all other stress components are zero, the proposed yield criterion becomes

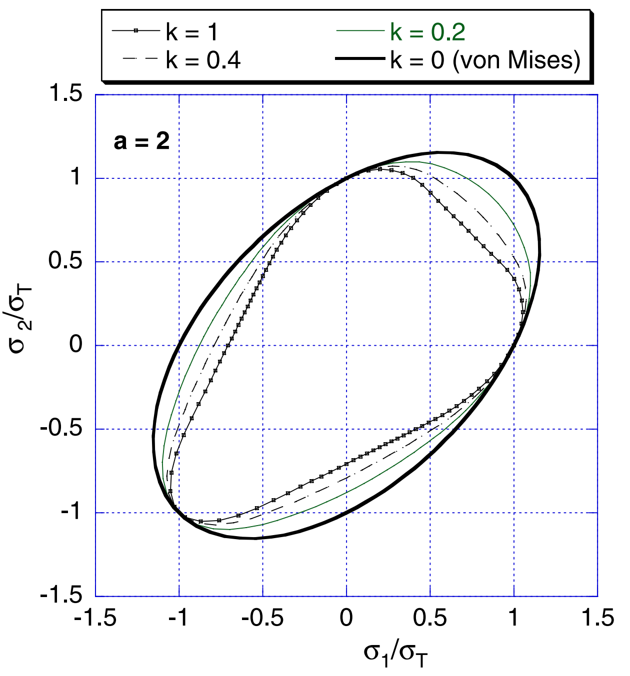

Fig. 2. Plane stress yield loci according to the proposed criterion (4) for different values of the ratio σ_T/σ_C between the yield stress in tension and compression, in comparison with the Von Mises yield locus.

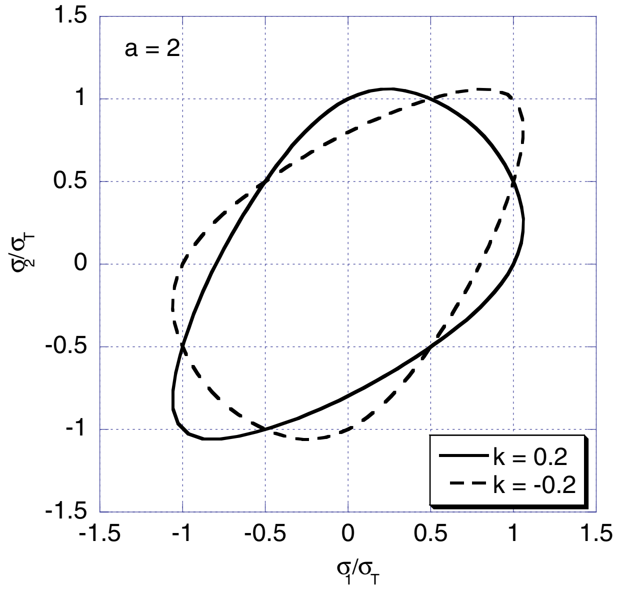

Fig. 3. Plane stress yield loci (4) corresponding to $\sigma_T/\sigma_C = 1.13(k = 0.2)$ and $\sigma_T/\sigma_C = 1/1.13$ $(k = -0.2)$.

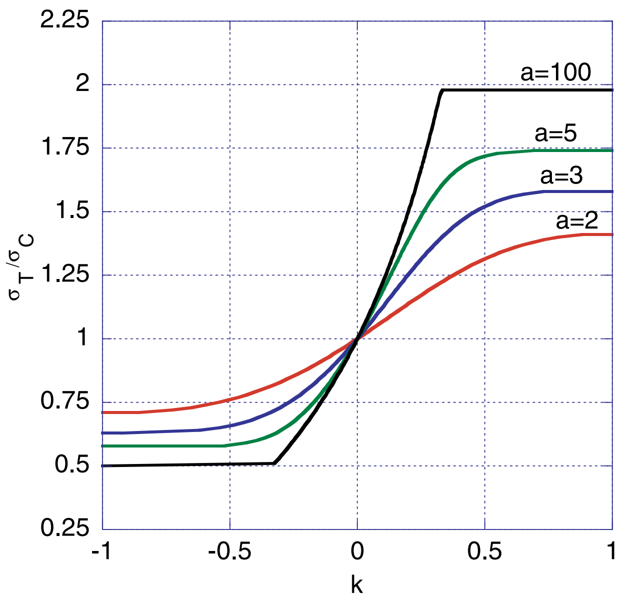

Fig. 4. The influence of the value of the parameter k on the ratio σ_T/σ_C of the uniaxial yield stress in tension and compression, for various values of the exponent a.

$$\left(\frac{\sigma}{6}+\sqrt{\frac{\sigma^2}{4}+\tau^2}\right)^a\cdot(1-k)^a+\left(\frac{\sigma}{6}-\sqrt{\frac{\sigma^2}{4}+\tau^2}\right)^a\cdot(1-k)^a+\left(\frac{\sigma}{3}\right)^a\cdot(1+k)^a=F. \tag{7}$$

Fig. 5 shows the representation in the tension–torsion plane $(\sigma/\sigma_T,\tau/\sigma_T)$ of the proposed yield loci corresponding to a fixed value of the parameter a $(a = 2)$ and several different values of k. Note the clear deviation from both Tresca and Mises criteria for k different from zero. Fig. 6 shows the representations in the deviatoric π plane (plane normal to the hydrostatic axis $\sigma_1 = \sigma_2 = \sigma_3$) of the proposed yield loci (4) for various values of the coefficient k between 0 and 1 and $a = 2$ (fixed), along with the von Mises and Tresca yield loci for comparison. As k increases, the ratio σ_T/σ_c is increasing and the yield loci depart drastically from the circular Von Mises locus.

As already mentioned, the analytic expression of the proposed yield criterion (4) was constructed based on the shape of the yield loci for randomly oriented cubic crystals deforming solely by twinning reported by Hosford and Allen (1973). These authors calculated these yield loci using an extension of the Bishop and Hill (1951) model, thus, assuming that the plastic strain of all crystals within a polycrystal is equal to the macroscopic strain. In view of comparison with the proposed analytic criterion (4), we calculated yield loci for randomly oriented cubic and hcp polycrystals using the one-site viscoplastic self-consistent polycrystal (VPSC) model of

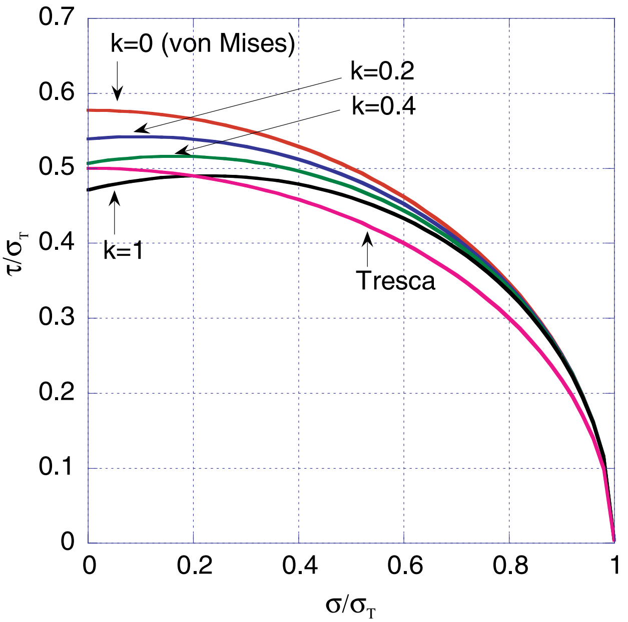

Fig. 5. Projections in the tension–torsion plane of the proposed yield loci (4) for various k-values and $a = 2$ (fixed), in comparison with Tresca and von Mises $(k = 0,\ a = 2)$ loci.

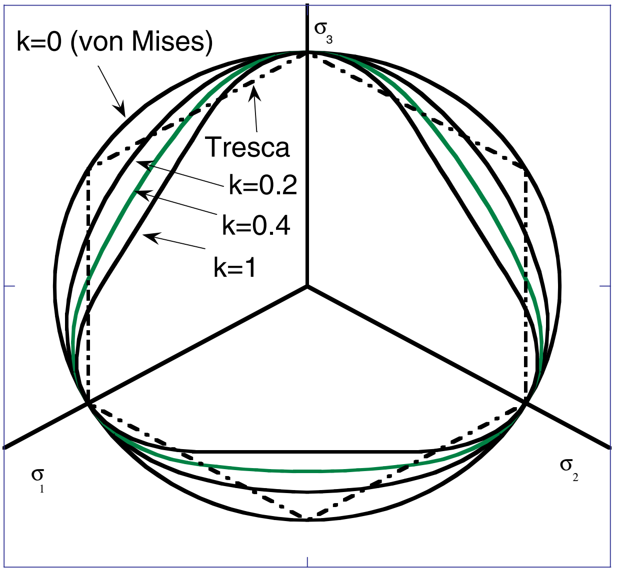

Fig. 6. Projection in the deviatoric π plane of the yield loci (4) for $a = 2$ and various values of k in comparison to Von Mises and Tresca loci.

Lebensohn and Tomé (see Lebensohn and Tomé, 1993) which assume a less rigid interaction between each grain and its surroundings (i.e., each grain is treated as an anisotropic, viscoplastic, ellipsoidal inclusion embedded in a uniform matrix which has the average constitutive behavior of the polycrystal).

First, let compare the yield loci obtained using the proposed criterion (4) with the yield loci for randomly oriented fee polycrystals deforming solely by $\{1\,1\,1\}\langle 1\,1\,\bar{2}\rangle$ twinning calculated using the VPSC model. The proposed yield condition (4) involves 2 parameters: the exponent a and the parameter k, which for a fixed is expressible solely in terms of the σ_T/σ_c ratio (see Eq. (5)). The VPSC model predicts a ratio of 0.83 between the yield stress in tension and compression (Hosford and Allen, 1973 reported a value of 0.78 for the same ratio). Assuming $a = 2$, we obtain $k = -0.3098$. Fig. 7(a) and (b) shows the yield stresses (open circles) obtained using the VPSC model and the projection of the yield locus predicted by the proposed criterion (4) for $k = -0.3098$ (solid line) in the biaxial plane and in the π plane, respectively. It is clearly seen that the proposed isotropic criterion describes very well the polycrystalline results. On the same figure are shown the comparison between the yield loci obtained with the VPSC model for randomly oriented bcc polycrystals deforming solely by $\{1\,1\,2\}\langle\bar{1}\,\bar{1}\,1\rangle$ twinning (solid circles) and the yield loci according to the proposed criterion (4) with $a = 2$ and for $k = 0.3098$ (which correspond to a ratio between the yield stress in tension and compression which is the reciprocal of the value corresponding to fcc polycrystals). Fig. 8(a) and (b) shows a comparison between the yield loci obtained using the proposed criterion (for $a = 3$ and $k = -0.0645$) with the yield loci for randomly oriented hcp Zr polycrystals deforming solely by tensile

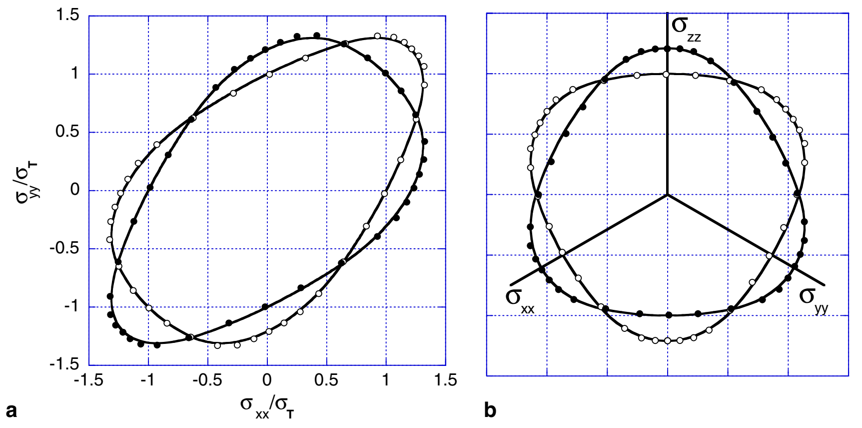

Fig. 7. Comparison between the VPSC yield locus for randomly oriented fcc (open circles) and bcc (closed circles) polycrystals deforming solely by twinning and the predictions of the proposed criterion (4): (a) in the biaxial plane; (b) in the π-plane.

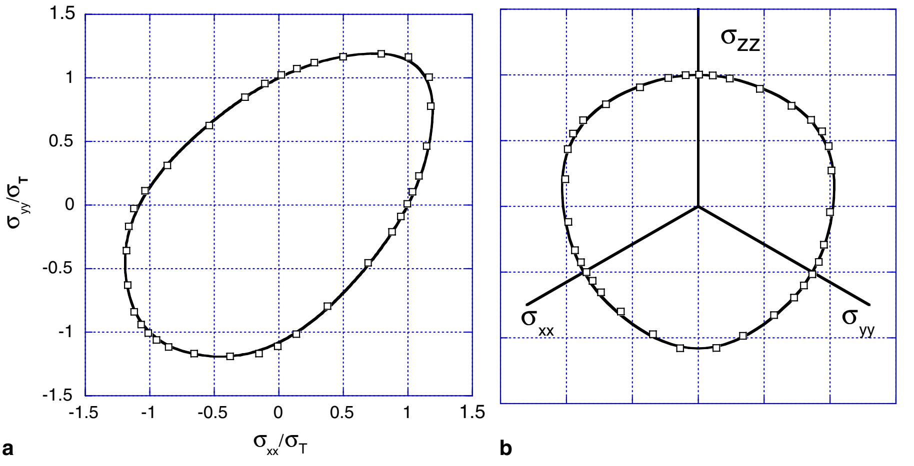

Fig. 8. Comparison between the VPSC yield locus for randomly oriented hcp Zr polycrystals deforming solely by twinning (open rectangles) and the predictions of the proposed criterion (4): (a) in the biaxial plane; (b) in the π-plane.

twinning $\{10\bar{1}2\}\langle 10\bar{1}1\rangle$ and compressive twinning $\{11\bar{2}2\}\langle 11\bar{2}\bar{3}\rangle$ calculated using the VPSC model. Again, the strength differential effect is very well captured.

3. Extension of the proposed isotropic yield criterion to include anisotropy

To describe both the asymmetry between tension and compression and the anisotropy observed in hcp metal sheets, we extend the proposed isotropic criterion (4) to orthotropy.

For the description of incompressible plastic anisotropy, Cazacu and Barlat (2001, 2003) introduced a general and rigorous method which is based on the theory of representation of tensor functions (Wang, 1970; Liu, 1982). It consists in substituting in the expression of any given isotropic criterion, the second and third invariants of the stress deviator with generalizations of these invariants compatible with the symmetry group of the material considered. However, with this approach, convexity is reinforced only numerically. For this reason, a particular case of this general theory, which is based on applying a 4th-order linear transformation operator on the Cauchy stress tensor, has received more attention (Sobotka, 1969; Barlat et al., 1991; Karafillis and Boyce, 1993; etc.). It is worth noting that by using the linear transformation approach, the convexity of the resulting anisotropic extension is automatically satisfied (Rockafellar, 1972).

To extend to orthotropy the proposed criterion (4), we use a linear transformation on the stress deviator $\boldsymbol{S}$, i.e., in the expression of the isotropic criterion (4), the principal values of the Cauchy stress deviator s_1,s_2,s_3 are substituted by the principal values of the transformed tensor Σ defined as

$$\Sigma = \boldsymbol{C}[\boldsymbol{S}], \tag{8}$$

where $\boldsymbol{C}$ is a constant 4th-order tensor. Thus, the proposed orthotropic criterion is of the form

$$(|\Sigma_1| - k \cdot \Sigma_1)^a + (|\Sigma_2| - k \cdot \Sigma_2)^a + (|\Sigma_3| - k \cdot \Sigma_3)^a = F, \tag{9}$$

where $\Sigma_1,\Sigma_2,\Sigma_3$ are the principal values of Σ. The only restrictions imposed on the tensor $\boldsymbol{C}$ are: (i) to satisfy the major and minor symmetries and (ii) to be invariant with respect to the orthotropy group. Thus, for 3-D stress conditions the orthotropic criterion involves 9 independent anisotropy coefficients; it reduces to the isotropic criterion (4) for $\boldsymbol{C}$ equal to the 4th-order identity tensor. It is worth noting that although the transformed tensor is not deviatoric, the orthotropic criterion is insensitive to hydrostatic pressure and thus the condition of plastic incompressibility is satisfied (proof is given in Appendix B). For $k \in [-1,1]$ and any integers $a \geqslant 1$, the anisotropic yield function is convex in the variables $\Sigma_1,\Sigma_2,\Sigma_3$ (principal transformed stresses).

Let $(\boldsymbol{x},\boldsymbol{y},\boldsymbol{z})$ be the reference frame associated with orthotropy. In the case of a sheet, $\boldsymbol{x}$, $\boldsymbol{y}$, and $\boldsymbol{z}$ represent the rolling, transverse, and the normal directions. Relative to the orthotropy axes $(\boldsymbol{x},\boldsymbol{y},\boldsymbol{z})$, the tensor $\boldsymbol{C}$ is represented by

$$\boldsymbol{C} = \begin{bmatrix} C_{11} & C_{12} & C_{13} & & & \\ C_{12} & C_{22} & C_{23} & & & \\ C_{13} & C_{23} & C_{33} & & & \\ & & & C_{44} & & \\ & & & & C_{55} & \\ & & & & & C_{66} \end{bmatrix}. \tag{10}$$

Since in the case of a thin sheet, the only non-zero stress components are the in-plane stresses $(\sigma_{xx},\sigma_{yy},\sigma_{xy})$, the principal values of Σ are:

$$
\begin{aligned}
\Sigma_1 &= \frac{1}{2}\left(\Sigma_{xx} + \Sigma_{yy} + \sqrt{(\Sigma_{xx} - \Sigma_{yy})^2 + 4\Sigma_{xy}^2}\right),\\
\Sigma_2 &= \frac{1}{2}\left(\Sigma_{xx} + \Sigma_{yy} - \sqrt{(\Sigma_{xx} - \Sigma_{yy})^2 + 4\Sigma_{xy}^2}\right),\\
\Sigma_3 &= \Sigma_{zz},
\end{aligned}
\tag{11}
$$

where

$$
\begin{aligned}
\Sigma_{xx} &= \left(\frac{2}{3}C_{11} - \frac{1}{3}C_{12} - \frac{1}{3}C_{13}\right)\sigma_{xx} + \left(-\frac{1}{3}C_{11} + \frac{2}{3}C_{12} - \frac{1}{3}C_{13}\right)\sigma_{yy},\\
\Sigma_{yy} &= \left(\frac{2}{3}C_{12} - \frac{1}{3}C_{22} - \frac{1}{3}C_{23}\right)\sigma_{xx} + \left(-\frac{1}{3}C_{12} + \frac{2}{3}C_{22} - \frac{1}{3}C_{23}\right)\sigma_{yy},\\
\Sigma_{zz} &= \left(\frac{2}{3}C_{13} - \frac{1}{3}C_{23} - \frac{1}{3}C_{33}\right)\sigma_{xx} + \left(-\frac{1}{3}C_{13} + \frac{2}{3}C_{23} - \frac{1}{3}C_{33}\right)\sigma_{yy},\\
\Sigma_{xy} &= C_{66}\sigma_{xy}.
\end{aligned}
$$

If σ_0^{T} and σ_0^{C} define the yield stress in tension and compression along the rolling direction $\boldsymbol{x}$, according to the proposed orthotropic criterion (9) it follows that:

$$
\begin{aligned}
\sigma_0^{\mathrm{T}} &= \left\{\frac{F}{[|\Phi_1| - k\Phi_1]^a + [|\Phi_2| - k\Phi_2]^a + [|\Phi_3| - k\Phi_3]^a}\right\}^{\frac{1}{a}},\\
\sigma_0^{\mathrm{C}} &= \left\{\frac{F}{[|\Phi_1| + k\Phi_1]^a + [|\Phi_2| + k\Phi_2]^a + [|\Phi_3| + k\Phi_3]^a}\right\}^{\frac{1}{a}},
\end{aligned}
$$

where

$$
\begin{aligned}
\Phi_1 &= \left(\frac{2}{3}C_{11} - \frac{1}{3}C_{12} - \frac{1}{3}C_{13}\right),\\
\Phi_2 &= \left(\frac{2}{3}C_{12} - \frac{1}{3}C_{22} - \frac{1}{3}C_{23}\right),\\
\Phi_3 &= \left(\frac{2}{3}C_{13} - \frac{1}{3}C_{23} - \frac{1}{3}C_{33}\right).
\end{aligned}
\tag{12}
$$

Similarly, if σ_{90}^{T} and σ_{90}^{C} are tensile and compressive yield stresses in the transverse direction, $\boldsymbol{y}$, then:

$$
\begin{aligned}
\sigma_{90}^{\mathrm{T}} &= \left\{\frac{F}{[|\Psi_1| - k\Psi_1]^a + [|\Psi_2| - k\Psi_2]^a + [|\Psi_3| - k\Psi_3]^a}\right\}^{\frac{1}{a}},\\
\sigma_{90}^{\mathrm{C}} &= \left\{\frac{F}{[|\Psi_1| + k\Psi_1]^a + [|\Psi_2| + k\Psi_2]^a + [|\Psi_3| + k\Psi_3]^a}\right\}^{\frac{1}{a}},
\end{aligned}
$$

where

$$\begin{aligned}\Psi_1 &= \left(-\frac{1}{3}C_{11}+\frac{2}{3}C_{12}-\frac{1}{3}C_{13}\right),\\ \Psi_2 &= \left(-\frac{1}{3}C_{12}+\frac{2}{3}C_{22}-\frac{1}{3}C_{23}\right),\\ \Psi_3 &= \left(-\frac{1}{3}C_{13}+\frac{2}{3}C_{23}-\frac{1}{3}C_{33}\right).\end{aligned} \tag{13}$$

Furthermore, yielding under pure shear parallel to the orthotropy axes occur when σ_{xy} is equal to

$$\tau^0 = \left\{\frac{F}{[|C_{66}|+kC_{66}]^a+[|C_{66}|-kC_{66}]^a}\right\}^{\frac{1}{a}}. \tag{14}$$

Yielding under equibiaxial tension occurs when σ_{xx} and σ_{yy} are both equal to

$$\sigma_b^T = \left\{\frac{F}{[|\Omega_1|-k\Omega_1]^a+[|\Omega_2|-k\Omega_2]^a+[|\Omega_3|-k\Omega_3]^a}\right\}^{\frac{1}{a}}, \tag{15}$$

while yielding under equibiaxial compression occurs when $\sigma_{xx}=\sigma_{yy}=\sigma_b^C$,

$$\sigma_b^C = \left\{\frac{F}{[|\Omega_1|+k\Omega_1]^a+[|\Omega_2|+k\Omega_2]^a+[|\Omega_3|+k\Omega_3]^a}\right\}^{\frac{1}{a}}, \tag{16}$$

where

$$\begin{aligned}\Omega_1 &= \left(\frac{1}{3}C_{11}+\frac{1}{3}C_{12}-\frac{2}{3}C_{13}\right),\\ \Omega_2 &= \left(\frac{1}{3}C_{12}+\frac{1}{3}C_{22}-\frac{2}{3}C_{23}\right),\\ \Omega_3 &= \left(\frac{1}{3}C_{13}+\frac{1}{3}C_{23}-\frac{2}{3}C_{33}\right).\end{aligned}$$

Furthermore, we assume that the plastic potential coincides with the yield function. Let denote by r_θ the Lankford coefficients (width to thickness strain ratios) under uniaxial tension in a direction at angle θ with the rolling direction. According to the proposed orthotropic criterion, it follows that:

$$\begin{aligned}r_0^T &= -\frac{(1-k)^a\Phi_1^{a-1}\Psi_1+(-1-k)^a(\Phi_2^{a-1}\Psi_2+\Phi_3^{a-1}\Psi_3)}{(1-k)^a\Phi_1^{a-1}(\Psi_1+\Phi_1)+(-1-k)^a(\Phi_2^{a-1}\Psi_2+\Phi_3^{a-1}\Psi_3+\Phi_2^a+\Phi_3^a)},\\ r_{90}^T &= -\frac{(1-k)^a\Psi_2^{a-1}\Phi_2+(-1-k)^a(\Psi_1^{a-1}\Phi_1+\Psi_3^{a-1}\Phi_3)}{(1-k)^a\Psi_2^{a-1}(\Phi_2+\Psi_2)+(-1-k)^a(\Psi_1^{a-1}\Phi_1+\Psi_3^{a-1}\Phi_3+\Psi_1^a+\Psi_3^a)},\\ r_0^C &= -\frac{(-1-k)^a\Phi_1^{a-1}\Psi_1+(1-k)^a(\Phi_2^{a-1}\Psi_2+\Phi_3^{a-1}\Psi_3)}{(-1-k)^a\Phi_1^{a-1}(\Psi_1+\Phi_1)+(1-k)^a(\Phi_2^{a-1}\Psi_2+\Phi_3^{a-1}\Psi_3+\Phi_2^a+\Phi_3^a)},\\ r_{90}^C &= -\frac{(-1-k)^a\Psi_2^{a-1}\Phi_2+(1-k)^a(\Psi_1^{a-1}\Phi_1+\Psi_3^{a-1}\Phi_3)}{(-1-k)^a\Psi_2^{a-1}(\Phi_2+\Psi_2)+(1-k)^a(\Psi_1^{a-1}\Phi_1+\Psi_3^{a-1}\Phi_3+\Psi_1^a+\Psi_3^a)}\end{aligned} \tag{17}$$

with Φ_1 to Φ_3 given by (12), Ψ_1 to Ψ_3 given by (13) and the superscripts T and C designating tensile and compressive states, respectively.

In the following, the proposed anisotropic criterion will be applied to the description of the anisotropy and asymmetry of the yield loci of textured polycrystalline magnesium and binary Mg–Th and Mg–Li alloys (data reported in Kelley and Hosford, 1968) and α (hcp) titanium (data after Lee and Backofen, 1966).

4. Applications to magnesium alloys

Kelley and Hosford (1968) reported the results of an experimental investigation into the anisotropy and asymmetry in yielding of textured polycrystalline binary Mg–Th (0.5% Th) and Mg–Li (4% Li) alloys. The data consists of the results of uniaxial compression tests in the rolling, transverse, and normal directions, respectively, uniaxial tensile tests in the rolling and transverse directions, as well as plane strain compression tests. Based on these data, the experimental yield loci corresponding to several constant levels (1%, 5%, and 10%) of the largest principal strain were reported (see Figs. 9 and 10 where experimental data are represented by symbols). Due to the strong basal pole alignment in the thickness direction, $\{10\bar{1}2\}$ twinning is easily activated by compression perpendicular to this direction, but is not active in tension within the plane. The effect of $\{10\bar{1}2\}$ twinning is clearly evident in the low compressive strengths at 1%. At 10% strain, the third quadrant strengths are compa-

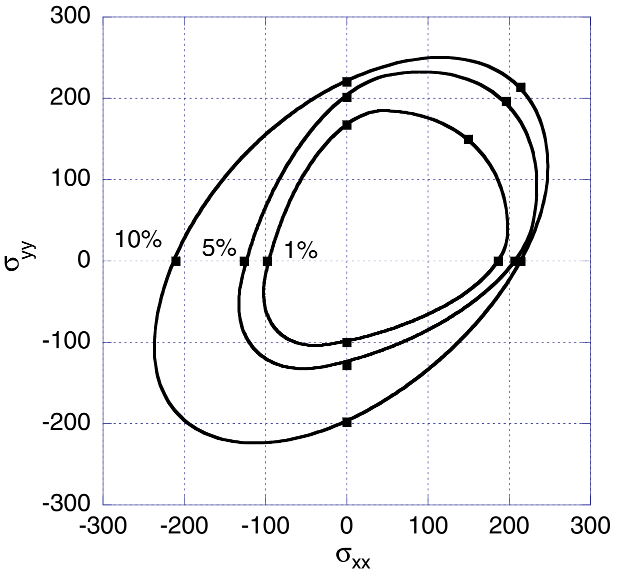

Fig. 9. Comparison between the plane stress yield loci ($\sigma_{xy} = 0$) for a Mg–0.5% Th sheet predicted by the proposed theory (solid lines) and experiments (symbols). Data after Kelley and Hosford (1968). Stresses in MPa.

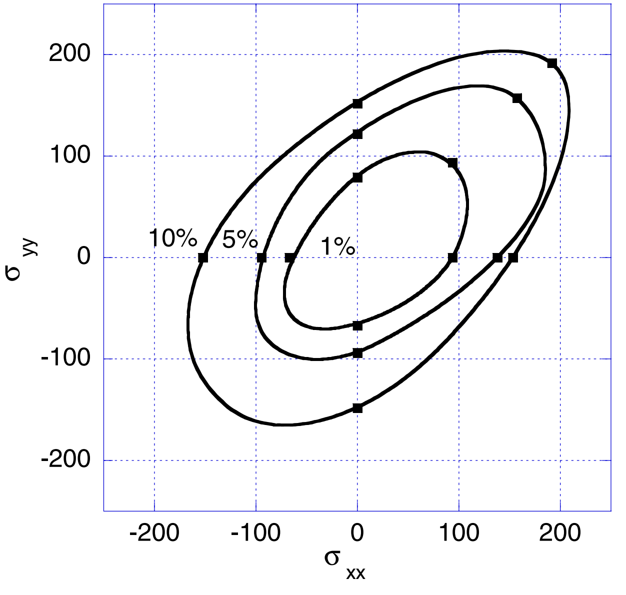

Fig. 10. Comparison between the plane stress yield loci ($\sigma_{xy} = 0$) for a Mg–4% Li sheet predicted by the proposed theory (solid lines) and experiments (symbols). Data after Kelley and Hosford (1968). Stresses in MPa.

rable to the first quadrant owing to the reorientations caused by $\{10\bar{1}2\}$ twinning which act to hinder further deformation processes. Fig. 9 shows the section of the theoretical yield loci (Eq. (9)) with $\sigma_3 = 0$ for Mg–Th together with the experimental data reported in Kelley and Hosford (1968). The anisotropy coefficients involved in the expression of the theoretical yield loci for biaxial stress states as well as the constant k were determined by least square fit using Eqs. (12), (13), and (15)–(17) and the data corresponding to the given strain level. The obtained values of these parameters corresponding to the 1%, 5%, and 10% surfaces are given in Table 1. No data were available for determination of the shear coefficients, C_{44}, C_{55}, and C_{66}. Note that the proposed theory reproduces very well the observed asymmetry in yielding.

The experimental yield loci for the Mg–Li alloy sheets are similar in shape to those for the Mg–Th alloy, but with much reduced yield stresses due to the occurrence of prism slip and to the weaker crystallographic texture. The effect of $\{10\bar{1}2\}$ twinning is evident in the low compressive strengths at 1% and 5% strains. Fig. 10 shows the theoretical yield loci for Mg–Li along with the data reported by

Table 1
Mg–Th coefficients

	k	C_{12}	C_{13}	C_{22}	C_{23}	C_{33}
1%	0.3539	0.4802	0.2592	0.9517	0.2071	0.4654
5%	0.2763	0.3750	0.0858	0.9894	0.0659	0.1238
10%	0.0598	0.6336	0.2332	1.4018	0.5614	0.7484

Table 2
Mg–Li coefficients

	k	C_{12}	C_{13}	C_{22}	C_{23}	C_{33}
1%	0.2026	0.5871	0.6975	0.9783	0.2840	0.1497
5%	0.2982	0.6103	0.8056	1.0940	0.5745	0.1764
10%	0.1763	0.5324	0.8602	1.0437	0.8404	0.2946

Kelley and Hosford (1968). The coefficients involved in the expressions of the theoretical yield loci are given in Table 2.

5. Applications to titanium 4A1–1/4 O_2

In the following, we apply the proposed orthotropic criterion to the description of the anisotropy and tension–compression asymmetry of 4A1–1/4 O_2 textured α (hcp) titanium alloy (data after Lee and Backofen, 1966). True stress–strain curves were reported for different loading paths: uniaxial tension in the ***x***-direction (rolling direction); uniaxial compression in the ***z***-direction (through-thickness compression), and plane strain compression in the ***z*** and ***y*** (transverse) directions. The material has nearly ideal basal texture with a deviation of about 25° from the sheet normal toward the transverse direction. Based on these data, the experimental yield loci corresponding to several constant levels of the largest principal strain were reported (see Fig. 11,

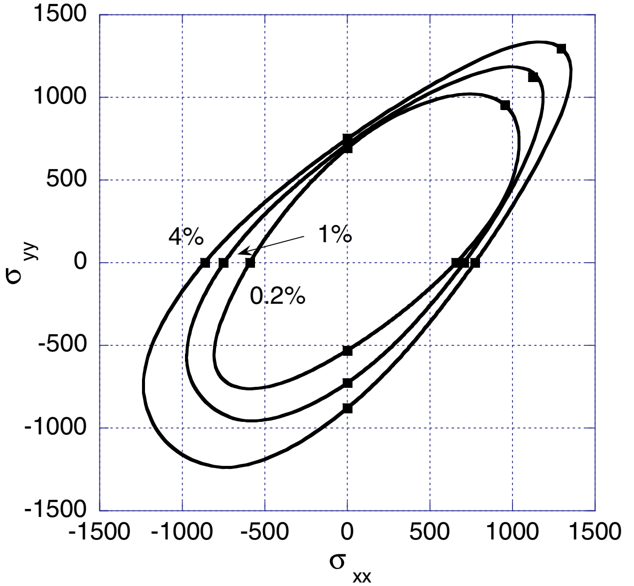

Fig. 11. Comparison between the plane stress yield loci ($\sigma_{xy} = 0$) for a 4A1–1/4 O_2 sheet predicted by the proposed theory (solid lines) and experiments (symbols). Data after Lee and Backofen (1966). Stresses in MPa.

experimental data are represented by symbols). Due to the strong basal pole alignment in the direction of the normal to the sheet, $\{10\bar{1}2\}$ twinning was activated by compression perpendicular to this direction, but is no twinning was revealed in tension testing within the plane (see Lee and Backofen, 1966). The effect of $\{10\bar{1}2\}$ twinning is clearly evident in the low compressive strengths in the rolling and transverse directions.

Fig. 11 also shows the theoretical yield loci along with the experimental data. The coefficients involved in the expressions of the theoretical yield loci are given in Table 3. Note the ability of the proposed criterion to correctly describe the asymmetry in yielding of 4Al–1/4O_2.

Table 3
4A1–1/4O_2 coefficients

	k	C_{12}	C_{13}	C_{22}	C_{23}	C_{33}
0.2%	0.1556	0.2285	0.0374	1.2967	0.2439	0.3422
1%	−0.1868	0.0431	0.3369	0.9562	0.3139	1.0861
4%	−0.2577	0.2178	0.3635	1.0422	0.3754	0.8825

Note: For all levels of effective plastic strain $a = 2$ and $C_{11} = 1.0$. The coefficients C_{44}, C_{55}, C_{66} were not determined.

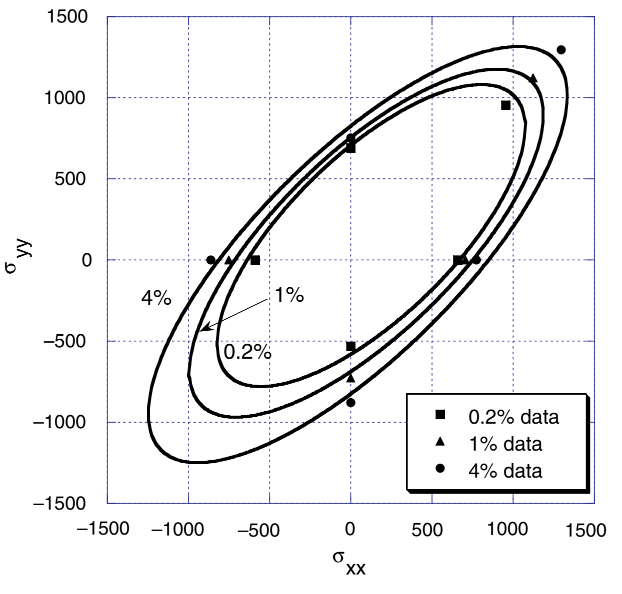

Fig. 12. Comparison between the plane stress yield loci ($\sigma_{xy} = 0$) for a 4A1–1/4O_2 sheet predicted by Hosford's (1966) modified Hill criterion (solid lines) and experiments (symbols). Data after Lee and Backofen (1966) (stresses in MPa).

In order to account for the eccentricity of the yield surfaces of titanium and its alloys, Hosford (1966) proposed a modification of the Hill criterion to include terms linear in stress

$$A\sigma_x + B\sigma_y + (-B - A)\sigma_z + F(\sigma_y - \sigma_z)^2 + G(\sigma_z - \sigma_x)^2 + H(\sigma_x - \sigma_y)^2 = 1. \quad (18)$$

Hosford's (1966) yield function given by Eq. (18) was applied to the same 4A1–1/4O_2 textured α (hcp) titanium alloy (see Fig. 12). Comparison between theoretical and experimental yield loci show that the proposed criterion (9) describes with greater accuracy the behavior near the biaxial tension state.

6. Summary and discussion

In this paper, a yield function describing both the tension/compression asymmetry and the anisotropic behavior of hcp metals and alloys in the full stress space was proposed. Anisotropy was introduced through a linear transformation on the deviatoric stress tensor. This yield function is convex, thus numerically robust and easily applicable to 3-D FE simulations of forming processes. For isotropic conditions, it reduces to a criterion with threefold symmetry which is expressed in terms of the principal values of the stress deviator and involves two parameters: parameter a, which gives the degree of homogeneity of the yield function and parameter k, which is expressible in terms of the ratio between the tensile and compressive yield strengths. If a is odd, for the yield function to be convex, the constant k must belong to a given numerical range: $[-1,1]$, while when a is even, the surface is convex irrespective of the values of k. This isotropic criterion reduces to von Mises when $k = 0$ and $a = 2$. It was shown that the isotropic criterion describes polycrystal yielding well.

For full 3-D stress conditions, the proposed orthotropic yield function involves 11 parameters, including 9 anisotropy coefficients along with k and a. The experimental characterization needed to obtain the material coefficients for this new yield function is relatively routine. It was shown that the proposed yield function appears to be suitable for the description of the strong asymmetry and anisotropy observed in textured binary Mg–Th and Mg–Li alloy sheets (data after Kelley and Hosford, 1968) and for 4A1–1/4O_2 titanium sheet (data after Lee and Backofen, 1966). Based on these results, it is believed that a very good description of the behavior for large strains can be obtained by using the proposed yield function for describing initial yielding and a hardening law that closely models the evolution of texture.

Acknowledgments

The authors thank Dr. Ricardo Lebensohn of Los Alamos National Laboratories for providing the VPSC code and for many helpful comments. Partial financial support for this work from NSF through Grant DMII-0322730 is gratefully acknowledged.

Appendix A. Proof of the convexity of the proposed isotropic yield function

The proposed isotropic yield condition is

$$f(S_1, S_2, S_3) = (|S_1| - kS_1)^a + (|S_2| - kS_2)^a + (|S_3| - kS_3)^a, \tag{A.1}$$

where S_i are the principal values of the stress deviator $\boldsymbol{S}$. We shall prove that for $k \in [-1,1]$ and any integer $a \geqslant 1$, this yield function is convex.

For the yield function to be convex, its Hessian matrix ought to be positive semi-definite.

Let H the Hessian matrix, i.e.,

$$H_{ij} = \frac{\partial^2 f}{\partial \sigma_i \partial \sigma_j}, \tag{A.2}$$

where $i,j = 1 \ldots 3$ and σ_i are the principal stresses. Isotropy dictates threefold symmetry of the yield surface, thus, it is sufficient to prove its convexity for stress states corresponding to $\sigma_1 \geqslant \sigma_2 \geqslant \sigma_3$.

If $\sigma_1 \geqslant \sigma_2 \geqslant \sigma_3$, it follows that:

$$\begin{aligned}
S_1 &= 2\cos(\alpha_1)\sqrt{\frac{J_2}{3}}, \\
S_2 &= 2\cos\left(\alpha_1 - \frac{2\pi}{3}\right)\sqrt{\frac{J_2}{3}}, \\
S_3 &= 2\cos\left(\alpha_1 + \frac{2\pi}{3}\right)\sqrt{\frac{J_2}{3}},
\end{aligned} \tag{A.3}$$

where α_1 is the angle satisfying $0 \leqslant 3\alpha_1 \leqslant \pi$ and whose cosine is given by: $\cos(3\alpha_1) = \frac{J_3}{2}\left(\frac{3}{J_2}\right)^{\frac{3}{2}}$, where J_2 and J_3 are the second and third invariants of the stress deviator (see Malvern, 1969).

For $0 \leqslant \alpha_1 < \pi/6$: $S_1 > 0$, $S_2 < 0$, $S_3 < 0$, and:

$$\begin{aligned}
H_{11} &= \frac{a(a-1)}{9}\{4(1-k)^a S_1^{a-2} + (1+k)^a(-1)^a(S_2^{a-2} + S_3^{a-2})\}, \\
H_{22} &= \frac{a(a-1)}{9}\{(1-k)^a S_1^{a-2} + (1+k)^a(-1)^a(4S_2^{a-2} + S_3^{a-2})\}, \\
H_{33} &= \frac{a(a-1)}{9}\{(1-k)^a S_1^{a-2} + (1+k)^a(-1)^a(S_2^{a-2} + 4S_3^{a-2})\}, \\
H_{12} &= \frac{a(a-1)}{9}\{-2(1-k)^a S_1^{a-2} - (1+k)^a(-1)^a(2S_2^{a-2} - S_3^{a-2})\}, \\
H_{13} &= \frac{a(a-1)}{9}\{-2(1-k)^a S_1^{a-2} - (1+k)^a(-1)^a(-S_2^{a-2} + 2S_3^{a-2})\}, \\
H_{23} &= \frac{a(a-1)}{9}\{(1-k)^a S_1^{a-2} + (1+k)^a(-1)^a(-2S_2^{a-2} - 2S_3^{a-2})\}.
\end{aligned} \tag{A.4}$$

Note that $\sum_{j=1}^{3} H_{ij} = 0$, for any $i = 1 \ldots 3$. Thus, the determinant of H is zero and its principal values are λ_1, λ_2, and $\lambda_3 = 0$. Furthermore:

$$\mathrm{tr}(H) = \lambda_1 + \lambda_2 = \frac{6a(a-1)}{9}\left\{(1-k)^a S_1^{a-2} + (1+k)^a(-1)^a(S_2^{a-2} + S_3^{a-2})\right\},$$
$$\mathrm{tr}_2(H) = \lambda_1\lambda_2 = \frac{a^2(a-1)^2}{9}\Big[(1-k)^{2a}(S_1^2)^{a-2} + (1+k)^{2a}(S_2^2)^{a-2} + (1-k^2)^a(S_1)^{a-2}(-S_2)^{a-2} + 3(1-k^2)^a(S_1)^{a-2}(-S_3)^{a-2} + 3(1+k)^{2a}(-S_2)^{a-2}(-S_3)^{a-2}\Big].$$

Since $S_1 > 0$, $S_2 < 0$, $S_3 < 0$, it follows that for $k \in (-1,1)$ and any integer $a \geqslant 1$: $\mathrm{tr}(H) = \lambda_1 + \lambda_2 \geqslant 0$ and $\mathrm{tr}_2(H) = \lambda_1\lambda_2 \geqslant 0$, i.e., the Hessian is always positive semi-definite.

For $\pi/6 < \alpha_1 < \pi/3$:

$$\begin{aligned}
H_{11} &= \frac{a(a-1)}{9}\{(1-k)^a(4S_1^{a-2} + S_2^{a-2}) + (1+k)^a(-1)^a S_3^{a-2}\},\\
H_{22} &= \frac{a(a-1)}{9}\{(1-k)^a(S_1^{a-2} + 4S_2^{a-2}) + (1+k)^a(-1)^a S_3^{a-2}\},\\
H_{33} &= \frac{a(a-1)}{9}\{(1-k)^a(S_1^{a-2} + S_2^{a-2}) + 4(1+k)^a(-1)^a S_3^{a-2}\},\\
H_{12} &= \frac{a(a-1)}{9}\{-2(1-k)^a(S_1^{a-2} + S_2^{a-2}) + (1+k)^a(-1)^a S_3^{a-2}\},\\
H_{13} &= \frac{a(a-1)}{9}\{(1-k)^a(-2S_1^{a-2} + S_2^{a-2}) - 2(1+k)^a(-1)^a S_3^{a-2}\},\\
H_{23} &= \frac{a(a-1)}{9}\{(1-k)^a(S_1^{a-2} - 2S_2^{a-2}) - 2(1+k)^a(-1)^a S_3^{a-2}\}.
\end{aligned} \tag{A.5}$$

It follows that $\sum_{j=1}^{3} H_{ij} = 0$, for any $i = 1,\ldots,3$. Thus, the determinant of H is zero and

$$\mathrm{tr}(H) = \frac{6a(a-1)}{9}\left\{(1-k)^a(S_1^{a-2} + S_2^{a-2}) + (1+k)^a(-1)^a S_3^{a-2}\right\}$$
$$\mathrm{tr}_2(H) = \lambda_1\lambda_2 = \frac{a^2(a-1)^2}{9}\Big[(1-k^2)^a(S_2^2)^{a-2} + (1-k)^{2a}(S_2^2)^{a-2} + (1-k)^{2a}(S_1)^{a-2}(S_2)^{a-2} + 3(1+k)^{2a}(S_2)^{a-2}(-S_3)^{a-2} + 3(1+k)^{2a}(S_1)^{a-2}(-S_3)^{a-2}\Big].$$

Since $S_1 > 0$, $S_2 > 0$, $S_3 < 0$, it follows that for $k \in (-1,1)$ and any integer $a \geqslant 1$: $\mathrm{tr}(H) \geqslant 0$ and $\mathrm{tr}_2(H) \geqslant 0$.

Thus, for $k \in [-1,1]$ and any integer $a \geqslant 1$ the yield function is convex.

Appendix B. Proof of the insensitivity of the proposed orthotropic yield function to hydrostatic pressure

The proposed orthotropic yield condition is

$$g(\Sigma_1, \Sigma_2, \Sigma_3) = (|\Sigma_1| - k\Sigma_1)^a + (|\Sigma_2| - k\Sigma_2)^a + (|\Sigma_3| - k\Sigma_3)^a, \tag{B.1}$$

where Σ_i are the principal values of the transformed stress tensor Σ defined as

$$\Sigma = \boldsymbol{C}[\boldsymbol{S}],$$

where $\boldsymbol{C}$ is a constant 4th-order tensor and $\boldsymbol{S}$ is the deviator of the Cauchy stress tensor. Let $(\boldsymbol{x}, \boldsymbol{y}, \boldsymbol{z})$ be the reference frame associated with orthotropy. Thus,

$$\frac{\partial g}{\partial p} = \frac{\partial g}{\partial \Sigma_m}\frac{\partial \Sigma_m}{\partial \Sigma_{ij}}\frac{\partial \Sigma_{ij}}{\partial p}, \quad i, j, m = 1 \ldots 3, \tag{B.2}$$

where $p = \sigma_{mm}$ denotes the mean stress and the convention of summation of repeated indices is adopted.

We shall prove that $\frac{\partial \Sigma_{ij}}{\partial p} = 0$, hence $\frac{\partial g}{\partial p} = 0$, i.e., the condition of plastic incompressibility is satisfied.

Indeed, the transformed stress tensor Σ can be expressed as:

$$\Sigma = \boldsymbol{CS} = \boldsymbol{CT\sigma}, \tag{B.3}$$

where $\boldsymbol{T}$ denotes the 4th-order deviatoric projection that transforms a 2nd-order tensor in its deviator. Thus,

$$\frac{\partial \Sigma_{ij}}{\partial p} = L_{ijkl}\delta_{kl} = L_{ijkk}, \quad i, j, k = 1, \ldots, 3, \tag{B.4}$$

where $\boldsymbol{L} = \boldsymbol{CT}$ is the 4th-order orthotropic tensor that relates the transformed tensor Σ to the Cauchy stress σ.

Relative to (x,y,z), the tensor $\boldsymbol{C}$ is represented by

$$C = \begin{bmatrix} C_{11} & C_{12} & C_{13} & & & \\ C_{12} & C_{22} & C_{23} & & & \\ C_{13} & C_{23} & C_{33} & & & \\ & & & C_{44} & & \\ & & & & C_{55} & \\ & & & & & C_{66} \end{bmatrix}, \tag{B.5}$$

while $\boldsymbol{T}$ is given by

$$T = \frac{1}{3}\begin{bmatrix} 2 & -1 & -1 & & & \\ -1 & 2 & -1 & & & \\ -1 & -1 & 2 & & & \\ & & & 3 & & \\ & & & & 3 & \\ & & & & & 3 \end{bmatrix}.$$

In (B.5) we used the simplified contracted indices convention of Voigt ($C_{1111} \overset{\text{not}}{=} C_{11},\ C_{1122} \overset{\text{not}}{=} C_{12},\ C_{13} \overset{not}{=} C_{1133}$, etc.). It follows that the non-zero components of the 4th-order tensor $\boldsymbol{L}$ are:

$$L_{11} = 2C_{11} - C_{12} - C_{13},$$
$$L_{12} = -C_{11} + 2C_{12} - C_{13},$$
$$L_{13} = -C_{11} - C_{12} + 2C_{13},$$
$$L_{21} = 2C_{12} - C_{22} - C_{23},$$
$$L_{22} = -C_{12} + 2C_{22} - C_{23},$$
$$L_{31} = -C_{32} + 2C_{31} - C_{33},$$
$$L_{32} = -C_{31} + 2C_{32} - C_{33},$$
$$L_{33} = -C_{31} + 2C_{33} - C_{32}.$$

Hence, we obtain

$$\begin{cases} L_{11} + L_{12} + L_{13} = 0, \\ L_{21} + L_{22} + L_{23} = 0, \\ L_{31} + L_{32} + L_{33} = 0. \end{cases} \tag{B.6}$$

Remarks:

1. Although Σ is not deviatoric, the three restrictions on the components of $\boldsymbol{L}$ ensure that $\frac{\partial \Sigma_{ij}}{\partial p} = 0$ for any $i,j = 1,\ldots,3$.
2. $L_{ijkl} \neq L_{klij}$. Hence, it can be concluded that the transformation considered is more general than the transformation adopted by Karafillis and Boyce (1993) in which major symmetries of the linear operator are reinforced despite the fact that such conditions are not necessary for ensuring plastic incompressibility.
3. To capture anisotropy, Barlat et al. (2005) have proposed the following transformation on the stress deviator:

$$\Sigma = \widetilde{\boldsymbol{C}}\boldsymbol{S}, \tag{B.7}$$

where the orthotropic tensor $\widetilde{\boldsymbol{C}}$ is given by

$$\widetilde{\boldsymbol{C}} = \begin{bmatrix} 0 & -\widetilde{C}_{12} & -\widetilde{C}_{13} & & & \\ -\widetilde{C}_{21} & 0 & -\widetilde{C}_{23} & & & \\ -\widetilde{C}_{31} & -\widetilde{C}_{32} & 0 & & & \\ & & & \widetilde{C}_{44} & & \\ & & & & \widetilde{C}_{55} & \\ & & & & & \widetilde{C}_{66} \end{bmatrix}.$$

Note that the transformation proposed by Barlat et al. (2005) is equivalent to the transformation proposed in this paper. Indeed, using Eqs. (B.3) and (B.7) we obtain:

$$\begin{aligned}
\widetilde{C}_{12} &= C_{11} - C_{12}, \\
\widetilde{C}_{13} &= C_{11} - C_{13}, \\
\widetilde{C}_{21} &= C_{22} - C_{12}, \\
\widetilde{C}_{23} &= C_{22} - C_{23}, \\
\widetilde{C}_{31} &= C_{33} - C_{13}, \\
\widetilde{C}_{32} &= C_{33} - C_{23}.
\end{aligned} \tag{B.8}$$

References

Avedesian, M.M., Baker, H. (Eds.), 1999. Magnesium and Magnesium Alloys. ASM Speciality Handbook. ASM International, Metal Parks, OH.

Agnew, S.R., Duygulu, O., 2005. Plastic anisotropy and the role of non-basal slip in magnesium alloy AZ31B. Int. J. Plasticity 21, 1161–1193.

Barlat, F., Lege, D.J., Brem, J.C., 1991. A six-component yield function for anisotropic materials. Int. J. Plasticity 7, 693–712.

Barlat, F., Brem, J.C., Yoon, J.W., Chung, K., Dick, R.E., Lege, D.J., Pourboghrat, F., Choi, S.-H., Chu, E., 2003. Plane stress yield function for aluminum alloy sheet – Part I: Theory. Int. J. Plasticity 19, 1297–1319.

Barlat, F., Cazacu, O., Zyczkowski, M., Banabic, D., Yoon, J.W., 2004. Yield Surface Plasticity and Anisotropy. In: Continuum Scale Simulation of Engineering Materials. Wiley-VCH, Weinheim, pp. 145–178.

Barlat, F., Aretz, H., Yoon, J.W., Karabin, M.E., Brem, J.C., Dick, R.E., 2005. Linear transformation-based anisotropic yield functions. Int. J. Plasticity 21, 1009–1039.

Bishop, J.W.F., Hill, R., 1951. A theoretical deviation of the plastic properties of a polycrystalline face-centered metal. Phil. Mag. Ser. 42, 1298–1307.

Bron, F., Besson, J., 2004. A yield function for anisotropic materials application to aluminum alloys. Int. J. Plasticity 20, 937–963.

Cazacu, O., Barlat, F., 2001. Generalization of Drucker's yield criterion to orthotropy. Math. Mech. Solids 6, 613–630.

Cazacu, O., Barlat, F., 2003. Application of representation theory to describe yielding of anisotropic aluminum alloys. Int. J. Eng. Sci. 41, 1367–1385.

Cazacu, O., Barlat, F., 2004. A criterion for description of anisotropy and yield differential effects in pressure-insensitive metals. Int. J. Plasticity 20, 2027–2045.

Chin, G.Y., Mammel, W.L., Dolan, M.T., 1969. Taylor analysis for {1 1 1} ⟨1 1 2⟩ twinning and {1 1 1} ⟨1 1 0⟩ slip under conditions of axisymmetric flow. Trans. TMS-AIME 245, 383–388.

Hill, R., 1948. A theory of the yielding and plastic flow of anisotropic metals. Proc. Roy. Soc. London A193, 281–297.

Hosford, W.F., 1966. Texture strengthening. Met. Eng. Quarterly 6, 13–19.

Hosford, W.F., Allen, T.J., 1973. Twining and directional slip as a cause for strength differential effect. Met. Trans. 4, 1424–1425.

Hosford, W.F., 1993. The Mechanics of Crystals and Textured Polycrystals. Oxford University Press, New York.

Kaiser, F., Bohlen, J., Deitmar, K., Kainer, K.U., 2003. Anisotropic properties of magnesium sheet AZ31. Mat. Sci. Forum 419–422, 315–320.

Karafillis, A.P., Boyce, M.C., 1993. A general anisotropic yield criterion using bounds and a transformation weighting tensor. J. Mech. Phys. Solids 41, 1859–1886.

Kelley, E.W., Hosford, W.F., 1968. Deformation characteristics of textured magnesium. Trans. TMS-AIME 242, 654–661.

Kuwabara, T., Katami, C., Kikuchi, M., Shindo, T., Ohwue, T., 2001. Cup drawing of pure titanium sheet-finite element analysis and experimental validation. In: Proceedings of the Seventh International Conference on Numerical Methods in Industrial Forming Processes, Toyohashi, Japan, 18–20 June, p. 781.

Lebensohn, R.A., Tomé, C.N., 1993. A self-consistent anisotropic approach for the simulation of plastic deformation and texture development of poly crystals: application to zirconium alloys. Acta Metall. et Mater. 41, 2611–2624.

Lee, D., Backofen, W.A., 1966. An experimental determination of the yield locus for titanium and titanium-alloy sheet. TMS-AIME 236, 1077–1084.

Liu, S.I., 1982. On representations of anisotropic invariants. Int. J. Eng. Sci. 20, 1099–1109.

Malvern, L.E., 1969. Introduction to the Mechanics of a Continuous Medium. Prentice-Hall Inc., Englewood Cliffs, NJ.

Rockafellar, R.T., 1972. Convex Analysis. Princeton University Press, Princeton, NY.

Sobotka, Z., 1969. Theorie des plastischen Fliessens von anisotropen Körpern. Zeit. Angew. Math. Mech. 49, 25–32.

Staroselsky, A., Anand, L., 2003. A constitutive model for hcp materials deforming by slip and twinning: application to magnesium alloy AZ31B. Int. J. Plasticity 19, 1843–1864.

Takuda, H., Yoshii, T., Hatta, N., 1999. Finite-element analysis of the formability of a magnesium-based alloy AZ31 sheet. J. Mater. Process. Techn. 89–90, 135–140.

Tomé, C.N., Lebensohn, R.A., Kocks, U.F., 1991. A model for texture development dominated by deformation twinning: application to zirconium alloys. Acta Mater. 39, 2667–2680.

Tomé, C.N., Maudlin, P.J., Lebensohn, R.A., Kaschner, G.C., 2001. Mechanical response of zirconium-I. Derivation of a polycrystal constitutive law and finite element analysis. Acta Mater. 49, 3085–3096.

Tomé, C.N., Lebensohn, R.A., 2004. Self consistent homogenization methods for texture and anisotropy. In: Continuum Scale Simulation of Engineering Materials. Wiley-VCH, Weinheim, pp. 473–497.

Van-Houtte, P., 1978. Simulation of the rolling and shear texture of brass by the Taylor theory adapted for mechanical twinning. Acta Metall. 26, 591–604.

Wang, C.C., 1970. A new representation theorem for isotropic functions, Part I and II. Arch. Rat. Mech. An. 36, 166–223.